

An infrared study of the UV photolysis of chlorine nitrate trapped in various matrices at 11 K

Armelle De Saxce and Louise Schriver

Laboratoire de Physique Moléculaire et Applications, CNRS UPR 136, Université Pierre et Marie Curie, Tour 13, Bâtiment 76, 4, Place Jussieu, 75252 Paris Cedex 05, France

Received 30 June 1992; in final form 31 July 1992

Photolysis of matrix isolated chlorine nitrate in argon matrix assisted by reactive matrices (solid nitrogen and oxygen) at 11 K have been carried out by visible and ultraviolet light in the 800–250 nm range. The product identification and relative measurements of the species time evolution were made by Fourier transform infrared spectrometry. Below 300 nm, two main dissociation channels are evidenced leading to $\text{ClNO} + \text{O}_2$ and $\text{ClONO} + \text{O}$, respectively. Recombination cage processes occur in matrices and the obtained results partially differ from gas-phase studies but give information on possible photoreactions in such condensed phase systems as polar stratospheric cloud surfaces.

1. Introduction

The large losses of ozone over Antarctica observed in recent years have been explained by both meteorological mechanisms and catalytic chemical reactions promoted by large concentrations of Cl_x species present mainly as ClO [1]. At lower concentrations, active radicals NO_x [2] and BrO [3] have been also implicated. Chlorine nitrate, ClONO_2 , is produced by recombination between NO_2 and ClO radicals [4] and behaves as a temporary reservoir for the chain termination step in the chlorine oxide and nitrogen oxide depletion schemes. Its concentration (0.5–1 ppb at altitudes of 24 to 34 km) depends on its lifetime which is an important parameter in the stratospheric ozone budget. Two main stratospheric destruction processes for ClONO_2 have been reported: (i) solar photolysis, (ii) heterogeneous reactions with H_2O and HCl occurring on the particles composing the polar stratospheric clouds (PSCs) and which can be an important source of active chlorine atoms [5]. Studies of the gas phase with various

techniques have been performed to determine the precise photolysis routes of the ClONO_2 photodissociation. However results are apparently in variance. Two studies favored the $\text{ClONO} + \text{O}(^3\text{P})$ channel [6,7] whereas other investigators identified $\text{Cl} + \text{NO}_3$ as the primary path of ClONO_2 photolysis [8–11]. More recently Burrows et al. [12] have found evidence for both routes. In the gas phase, detailed knowledge of the photolytic decomposition channels is difficult to obtain because the products of all the stages of the reaction generally contribute to the analysis of the mixture. In this view, the matrix isolation technique coupled with FTIR spectroscopy is particularly well suited to the determination of primary products if the fragments formed from photolysis do not recombine to regenerate the precursor. The object of the present work was therefore to use this technique to explore the nature of the primary processes for ClONO_2 photodissociation. Studies were carried out in different matrices (Ar , N_2 , O_2) with different light sources and various filters between 250 and 800 nm.

Correspondence to: L. Schriver, Laboratoire de Physique Moléculaire et Applications, CNRS UPR 136, Université Pierre et Marie Curie, Tour 13, Bâtiment 76, 4, Place Jussieu, 75252 Paris Cedex 05, France.

2. Experimental

Chlorine nitrate was prepared by the reaction of

Cl_2O with N_2O_5 according to the method of Schmeisser [13]. Cl_2O was obtained by the reaction of chlorine with dry yellow mercury(II)oxide described by Cady [14]. Dinitrogen pentoxide was synthesized by the reaction of concentrated nitric acid with purified phosphorus(V)oxide following the procedure described by Gruenhut et al. [15]. The major impurity HNO_3 was removed by repeated pumping on the -60°C ClONO_2 condensate. Matrix samples M/ClONO_2 of mole ratio from 500 to 3000 were prepared using standard manometric procedures. Ar, N_2 and O_2 were obtained commercially with a purity of greater than 99% and used without further purification.

The studies were performed using a closed-cycle helium refrigerator Air Products model 202A with a rotating base which allowed us to place the sample either in front of the spectrometer beam or in a perpendicular direction in front of the photolysis sources through ICs or CaF_2 windows respectively. Matrix gases were decomposed onto a golden mirror maintained about at 20 K (Ar, O_2) or 17 K (N_2) with a deposition rate of about 10 mmol/h. Infrared spectra were recorded at 11 K by reflexion on a Bruker IRF 113V. Typically each spectrum consisted of an average of 100 scans. Most of the absorbance measurements were made over the range of 500–4000 cm^{-1} at a resolution of 0.5 cm^{-1} . Resulting frequency accuracies for absorption are estimated to be 0.1 cm^{-1} .

Studies of the photolysis of the matrix isolated chlorine nitrate were conducted using a medium pressure mercury lamp (93136 Philips, 90 W) or a xenon lamp (XC150S Cunow, 150 W). The sample was exposed either to the full or to filtered light obtained with Schott cutoff filters at 715 (RG715), 665 (RG665), 530 (OG530), 345 (WG345) and 280 nm (WG280). In order to prevent infrared irradiation and sample heating, a cell filled with water (5 cm long) was set between the lamp and the cryostat entrance.

3. Results

3.1. Vibrational spectra of ClONO_2 in matrices

A complete assignment of the infrared spectra in the gas and solid phases of ClONO_2 assuming a

planar heavy atom structure was first reported by Miller et al. [16]. Later, the planarity of chlorine nitrate was well established from microwave studies [17,18] and Raman and torsional spectra [19,20]. More recently high-resolution FTIR isolation spectra of chlorine nitrate in nitrogen and argon matrices were reported [21]. The two major lines observed at about 1730 and 1720 cm^{-1} were assigned to a Fermi resonance between ν_1 and the combination $\nu_2 + \nu_6$. In argon matrices all fundamentals showed a more complex structure, without significant temperature and concentration dependence, than in nitrogen matrices. We have recorded infrared spectra of ClONO_2 in Ar, N_2 , O_2 and mixed Ar– N_2 matrices at various matrix ratios. Our spectra were in good agreement with the previous studies, showing similar fundamental structure in the three types of matrices. As illustrated in fig. 1, some splittings previously observed by Griffith in argon could be due to nitrogen impurities. As soon as nitrogen was added in argon, new sharp lines successively appeared and grew up in all fundamental regions. The replacement of the monomer bands for various nitrogen rare gas ratios suggests formation of $(\text{N}_2)_n\text{-ClONO}_2$ aggregates inside the monoatomic crystal, and shows strong specific interactions between N_2 and ClONO_2 . The absorption lines with relative peak absorbances of the ClONO_2 monomer in the three types of matrices between 500 and 2000 cm^{-1} at a temperature of 11 K are listed in table 1.

3.2. Photolysis in argon matrix

An initial study of the photolysis of a ClONO_2/Ar sample (1/500) was performed with the Xenon lamp and the various filters as described in section 2. At a wavelength longer than 320 nm there is no evidence for product formation after 10 h irradiation time with each filter; also the relative intensities of ClONO_2 bands remained unchanged. This observation agrees with the ClONO_2 ultraviolet spectrum in which the absorption between 3500 and 4600 Å is weak [22]. Subsequent experiments were therefore conducted using a medium pressure mercury lamp ($250 < \lambda < 800$ nm) either without filter or only with the WG280 cutoff filter.

Full irradiation of a ClONO_2/Ar (1/3000) sample for 32 h revealed a depletion on the ClONO_2

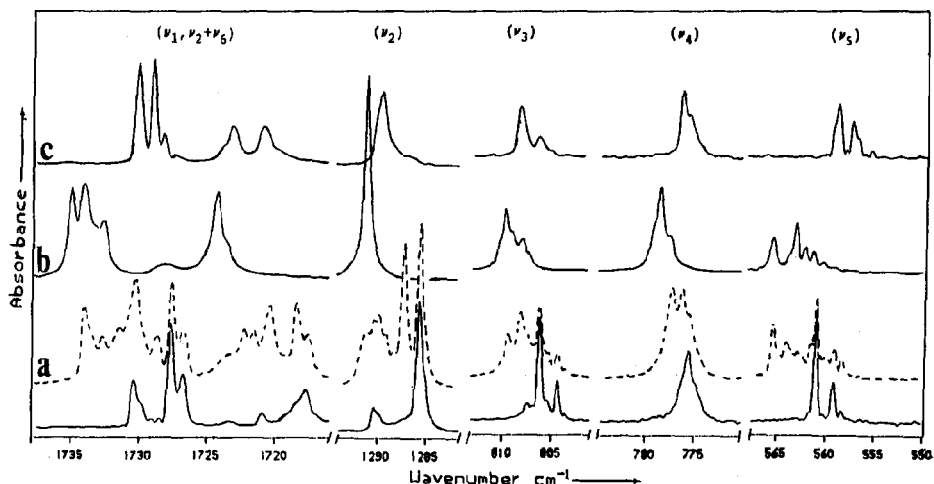


Fig. 1. Expanded FTIR spectra, recorded at 11 K, of ClONO_2 fundamentals in various matrices. (a) In argon ($M/R=3000$); (—) pure argon, (---) argon containing 1% nitrogen. (b) In nitrogen ($M/R=500$). (c) In oxygen ($M/R=3000$). Ordinate scales are the same for each region of the same spectrum but different for each spectrum.

molecule of only 15%. The major new product bands were observed at 1804.9 and 585.0–584.3 cm^{-1} as illustrated in fig. 2A. These bands can be assigned unambiguously to the CINO molecule from its spectrum recorded in argon by Jones et al. [23]. Other numerous weak bands were also observed after irradiation; they were mainly due to the photolysis of impurity traces such as HNO_3 as shown by Cheng et al. [24]. Careful analysis led to the observation of only three new weak lines assignable to ClONO_2 photoproducts and which appeared at 1877.0, 1799.8–1799.1 and 1600.2 cm^{-1} . The first one is indicative of NO formation [25] whereas the doublet 1799.8–1799.1 cm^{-1} can be due to a CINO molecule perturbed by other partners in the matrix cage. The 1600.2 cm^{-1} feature did not seem assignable to water impurity and will be discussed later. Frequencies and assignments for all new bands are listed in table 2. Fig. 3A shows the concentration time profile for ClONO_2 and CINO products obtained from optical density measurements of one well defined product absorption for each species. The decay of ClONO_2 molecules was fitted by a first-order reaction expression:

$$A_{\text{ClONO}_2}^t = A_{\text{ClONO}_2}^0 \exp(-k_1 t), \quad (1)$$

and led to a pseudo rate constant $k_1 = (1.4 \pm 0.3)$

$\times 10^{-4} \text{ min}^{-1}$ in this experiment. The corresponding growth curves of CINO and NO products are exponential but with a different behaviour: the NO reached a constant value at short times whereas the CINO continued to increase. In the absence of secondary reactions the amount of CINO generated in time t (A_{CINO}^t) would be given, in a first approximation, by

$$A_{\text{CINO}}^t = A_{\text{CINO}}^\infty [1 - \exp(-k_2 t)], \quad (2)$$

where A_{CINO}^∞ refers to the CINO absorption intensity at infinite time corresponding to the total depletion of ClONO_2 . We have attempted to estimate the A_{CINO}^∞ value from the experimental ratio $A_{\text{CINO}}^t / (A_{\text{ClONO}_2}^0 - A_{\text{ClONO}_2}^t)$, which was found to be constant at each time and equal to 1.5 for the absorption at 1805 (CINO) and 1285.8 cm^{-1} (ClONO_2). In this way the experimental CINO growth curve of fig. 3A is well fitted by expression (2) and led to a k_2 value of $(1.6 \pm 0.3) \times 10^{-4} \text{ min}^{-1}$ similar to that observed for the ClONO_2 depletion in the same experiment.

One irradiation experiment was also performed using the WG280 cutoff filter. Similar product bands were observed although the efficiency of the photolysis was much smaller than that without the filter.

Table 1

Normal mode vibrational frequencies (cm^{-1}) for ClO'NO₂ in various matrices. Relative peak absorbances (in brackets) are normalized to ν_2 in argon (1285.8 cm^{-1}) and nitrogen (1291.4 cm^{-1}) matrices and to ν_1 (1730.0 cm^{-1}) in the oxygen matrix

Argon	Argon/nitrogen ^{a)} 1/100	Nitrogen	Oxygen	Normal mode
	1734.0			NO ₂ a-stretching (ν_1)
	1732.7			
1730.3 (36.1)	1731.4	1735.0 (46.1)	1730.0 (100)	
	1728.7			Fermi resonance with ($\nu_2 + \nu_6$)
1727.6 (79.4)		1734.0 (48.3)	1729.0 (98.9)	
1726.7 (40.5)		1732.7 (29.9)	1728.2 (25.9)	
	1722.3			Fermi resonance with ($\nu_2 + \nu_6$)
	1721.6			
1720.9 (10.9)		1728.2 (7.1)	1723.2 (39.6)	
	1720.3			NO ₂ s-stretching (ν_2)
	1718.4			
1717.8 (28.5)		1724.3 (43.9)	1720.9 (31.1)	
	1291.4			NO ₂ s-stretching (ν_2)
	1287.4			
1285.8 (100)		1291.4 (100)	1289.7 (71.9)	
	809.4			O'-Cl stretching (ν_3)
	808.0			
801.6 (40.6)		809.7 (20.9)	808.1 (25.0)	
804.3 (15.7)		808.0 sh	806.2 (10.0)	
	777.3			ONO scissoring (ν_4)
775.6 (27.6)		778.6 (27.9)	776.3 (33.1)	
		777.5 (11.9)	775.6 (20.0)	
710.8 (4.1)		708.4 (3.6)	710.0 (5.6)	NO ₂ wagging (ν_5)
702.3 (0.9)			704.6 (9.1)	
	565.4			NO ₂ rocking (ν_5)
	564.1			
560.9 (43.5)		563.2 (14.9)	559.0 (27.5)	
559.1 (15.7)		561.3 (6.2)	557.6 (14.8)	
433.6 ^{b)}		434.9 ^{b)}	433.1 ^{b)}	NO' stretching (ν_6)

^{a)} Only bands due to (N₂)_n-ClONO₂ aggregates are reported.

^{b)} Normal mode ν_6 was not observed but calculated without anharmonicity correction from the overtone $2\nu_6$ found at 867.1 cm^{-1} in argon, 869.8 cm^{-1} in nitrogen and 866.2 cm^{-1} in oxygen matrix.

3.3. Photolysis in nitrogen matrix

Exposure of ClONO₂/N₂ samples (1/500) to full irradiation over 42 h depleted the matrix by about 20% in ClONO₂ and produced three pattern absorptions about 2235, 1820 and 585 cm^{-1} and other weaker features at 1874.3 and 1602.8 cm^{-1} which are summarized in table 2. The matrix also contained traces of HNO₃ impurity trapped from the gas phase. The strongest line at 1819.1 cm^{-1} with shoul-

ders at 1817.2 and 1814.3 cm^{-1} correlated to the weak 584.3–583.4 cm^{-1} doublet is assigned to the ClNO molecule whose absorptions are expected to exhibit a shift from those recorded in argon matrix. A weak bulky structure centered at 2235 cm^{-1} suggested formation of N₂O, on the basis of its infrared spectrum recorded in nitrogen matrix [26], although the ν_1 absorption, expected about 1291 cm^{-1} , was unfortunately not observed due to the interference with the ClONO₂ ν_2 band. The weak band at

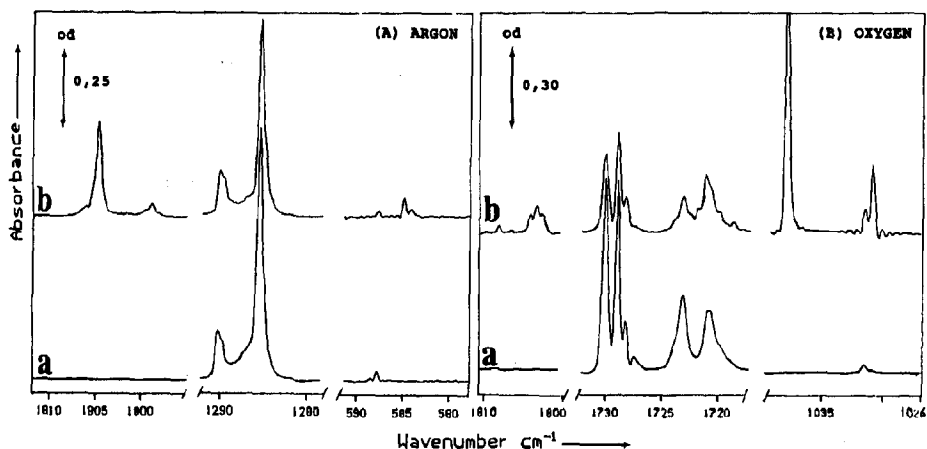


Fig. 2. FTIR spectra (a) before photolysis and (b) after photolysis (with a medium pressure mercury lamp) of ClONO_2 in various matrices. (A) illustrates ClNO formation in argon matrix ($M/R=3000$) after 32 h of irradiation without filter. (B) illustrates ClNO and O_3 formation in oxygen matrix ($M/R=3000$) after 26 h of irradiation with the WG280 cutoff filter. Relative ClONO_2 decay is indicated by the ν_2 band (1285.8 cm^{-1}) in argon and by the ν_1 bands (1730.0 and 1729.0 cm^{-1}) in oxygen.

585.4 cm^{-1} could correspond to the ν_2 mode of N_2O reported at 589 cm^{-1} . The weak band located at 1874.3 cm^{-1} is due to NO [27]. Time evolution of ClONO_2 , ClNO and N_2O product bands during photolysis was followed by integrated intensity measurements of the 778.6 cm^{-1} ClONO_2 band, the 1819.1 cm^{-1} ClNO band and the 2235.3 cm^{-1} N_2O band. The growth of ClNO and N_2O was correlated with the destruction of ClONO_2 molecules. Using the same procedure as for the argon matrix, first-order rate constants k_1 and k_2 were calculated and found to be similar, equal to about $(7.3 \pm 0.4) \times 10^{-5}\text{ min}^{-1}$ in the given experiment.

3.4. Photolysis in oxygen matrix

Direct formation of ozone from the photolysis of pure solid oxygen occurred with the unfiltered medium pressure mercury lamp but was prevented using the WG280 cutoff filter. In consequence, photolysis of ClONO_2 in an oxygen matrix was performed with filtered light. Product absorption regions of special interest in the spectra of a $\text{ClONO}_2/\text{O}_2$ sample ($1/3000$) before photolysis and after 26 h of irradiation with the filtered medium pressure mercury lamp are shown in fig. 2B. A higher loss of ClONO_2 than in the argon and nitrogen matrices was observed with a richer product spectrum. The po-

sition and peak optical densities of the new absorptions are summarized in the third column of table 2. Consistent with the previous observations in argon and nitrogen, the presence of ClNO was evidenced at 1803.8 and 590.8 cm^{-1} . Prominent bands due to ozone were clearly observed at 1037.8 and 1030.8 cm^{-1} with weaker bands at 2108.3 , 2096.2 , 702.6 and 697.8 cm^{-1} . Other features at 1676.6 , 1316.2 , 1265.2 , 786.9 and 778.9 cm^{-1} corresponded reasonably well with the fundamentals of ClNO_2 isolated in argon matrix [28]. Under prolonged photolysis a new band, previously obscured by the parent ClONO_2 absorption, was growing at 1721.1 cm^{-1} ; this band, corresponding with a weaker one at 857.2 cm^{-1} , can be assigned to the ClONO species on the basis of literature data [28]. Weak peaks at 1866.2 , 1752.0 and 1436.1 cm^{-1} were probably due respectively to NO [29], OCINO [28] and the ClOO radical [30]. Some other photoproduct features at 1302.7 , 1286.5 and 880.3 cm^{-1} were discernible but remain unidentified. Fig. 3B displays the time evolution of typical bands of ClONO_2 , ClNO and O_3 as recorded in a typical irradiation study over 26 h. Growth of ClNO and O_3 seems to be correlated with the ClONO_2 decay, but ClNO absorption band intensity approaches a limit after about 13 h of irradiation. Deviation from expression (2) was observed for O_3 and ClNO growth indicating the occurrence of secondary reactions, as discussed later.

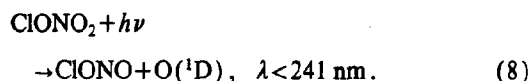
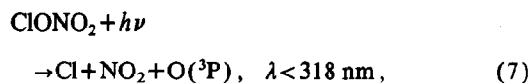
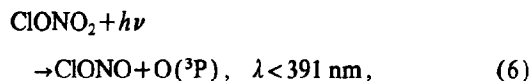
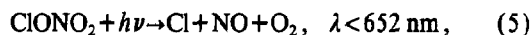
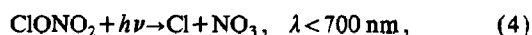
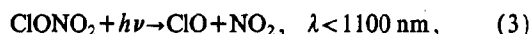
Table 2

Infrared frequencies (cm^{-1}) and peak absorbances (in brackets) of absorptions observed following photolysis of ClONO_2 samples in various matrices. These results were obtained after an irradiation time of 32 h in argon, 42 h in nitrogen and 26 h in oxygen. The photolysis was performed with a medium pressure mercury lamp, without a filter for the argon matrix and with the WG280 cutoff filter for the oxygen matrix

Argon	Nitrogen	Oxygen	Assignment	Argon	Nitrogen	Oxygen	Assignment
	2241.7 (0.02)		N_2O			1439.7 sh	ClOO
	2236.9 (0.04)					1436.1 (0.05)	
	2235.3 (0.04)		ClONO_2			13.16.2 (<0.01)	
	2234.0 (0.03)					1302.7 (0.04)	
	2232.4 sh					1300.0 sh	
		2108.3 (0.03)	O_3			1287.2 sh	
		2096.2 (0.01)				1286.5 (0.07)	
1877.0 (0.05)	1874.3 (0.03)	1866.2 (0.06)	NO			1265.2 (0.02)	ClONO_2
						1262.8 sh	
1806.3 (0.03)	1819.1 (0.18)	1804.5 sh	ClNO			1037.8 (0.88)	O_3
1804.9 (0.28)	1817.2 sh	1803.8 (0.10)				1030.8 (0.24)	
1799.8 (0.02)	1814.3 sh	1803.1 sh				880.3 (0.06)	
1799.1 (0.04)						857.2 (0.03)	ClONO
		1752.0 (0.01)	OCINO			786.9 (0.02)	ClONO_2
		1721.9 sh				778.9 sh	
		1721.1 (0.20)	ClONO			702.6 (0.04)	O_3
		1719.9 sh			697.8 (0.03)		
		1718.7 sh					
		1676.6 (0.03)	ClONO_2				
		1675.6 (0.04)					
1600.2 (0.02)	1602.8 (0.02)				586.6 (0.01)		N_2
1599.5 (0.01)			O_2		585.4 (0.03)		
				585.0 (0.06)	584.3 (0.03)	590.8 (0.02)	ClNO
				584.3 (0.02)	583.4 sh	589.9 sh	

4. Discussion

Several photolysis reactions are available for ClONO_2 :



The ClONO_2 photolytic process is assumed to be the same in the three matrices but in the reactive matrices (O_2 and N_2) formation of product reactions between atoms or radicals and matrix molecules can be expected. Thus the following overall observations have to be taken in account:

(i) Formation of ClNO product occurs in the three matrices, which appears to correlate with the ClONO_2 decay except in the oxygen matrix where the ClNO growth reaches an asymptotic limit at shorter times.

(ii) Identification of N_2O product in the nitrogen matrix, which results from the combination of nitrogen molecules with oxygen atoms in excited states produced during the matrix photolysis [31].

(iii) Detection of ClONO , OCINO , ClONO_2 and O_3 products only in the oxygen matrix. The ozone for-

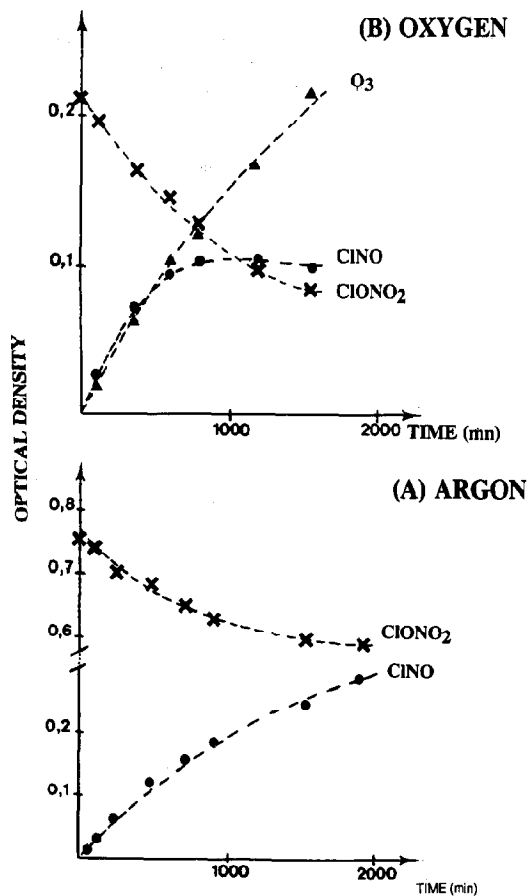


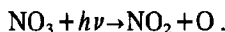
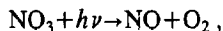
Fig. 3. Absorbance versus photolysis time plot for (A) CINO (1804.9 cm^{-1}) growth and ClONO₂ (1235.8 cm^{-1}) decay in argon matrix ($M/R=3000$). The photolysis was performed with a medium pressure mercury lamp without filter. (B) CINO (1803.8 cm^{-1}) and O₃ (1030.8 cm^{-1}) growth and ClONO₂ (776.3 cm^{-1}) decay in oxygen matrix ($M/R=3000$). The photolysis was performed with a medium pressure mercury lamp with the WG280 cutoff filter.

mation is indicative of the production of oxygen atoms in the triplet state but it does not prove that O(³P) is the initial photolysis product because of the possibility of the rapid quenching of O(¹D) by O₂ molecules.

Mechanisms consistent with these observations are now discussed. Stabilization of CINO in the present experiments seem to provide evidence for the occurrence of the primary photolysis process (5) leading to the formation of Cl+NO followed by cage recombination of the radical products in the site of their

photoproduction. This scheme is consistent with the appearance of NO traces in all the matrices and with ClOO radical formation in the oxygen matrix, the produced atomic chlorine being able to react with a nearby oxygen molecule [29].

However, the possibility that CINO could be formed indirectly from path (4) (the channel observed in the gas phase) cannot be ruled out although no absorption assignable to NO₃ species was observed in all matrices. The nitrate radical has important absorption cross sections between 570 and 670 nm and two possible sets of photodissociation products can occur in the gas phase [32]:



In a matrix cage, the first path of this scheme followed by a recombination process involving a Cl atom and produced NO, could also explain the observation of CINO in the matrices.

The particular behaviour of CINO growth in the oxygen matrix can be explained by photolysis of CINO in solid oxygen which produces chlorine nitrate as reported by Tevault and Smardzewski [33]. CINO formation also involves the production of molecular oxygen. As reported by Cairns and Pimentel [34] solid oxygen shows two absorptions, a sharp feature near 1549 cm^{-1} and a broader band near 1605 cm^{-1} due to a combination involving translational lattice modes. Thus, the appearance of a weak band at about 1600 cm^{-1} in argon and nitrogen matrices after photolysis could be an indication of oxygen formation.

The oxygen atom and ClONO molecule identified in oxygen matrices may be formed either by channel (6) (ClONO₂→CINO+O(³P)) or by channel (8) (ClONO₂→CINO+O(²D)) although the last one could be inconsistent above 280 nm irradiation. The possibility of rapid quenching of O(³P) by oxygen molecules does not allow us to accurately determine the dominant photochemical pathway. However, the obtained data in nitrogen matrices give additional information. The weakness of N₂O formation observed without a filter suggests that O(¹D) atoms cannot be produced in significant amounts in the photolysis of the ClONO₂/O₂ matrix. Thus, pathway (6) does indeed occur in good agreement with ear-

lier data from the gas phase and under our irradiation conditions, pathway (8) appears as a minor channel. The observation, in an oxygen matrix, of OCINO and CINO₂ species together with the CIONO product can be explained, from previous work [28], by the photolysis behavior of the CIONO molecule which undergoes intramolecular rearrangement in the matrix cage to produce the more stable CINO₂ isomer via a two-step process which involves the OCINO molecule as an intermediate. Pathways (6) and (8) were not evidenced in the argon matrix indicating that, in such a matrix, a cage recombination between CIONO and O occurs.

The experiments described above clearly demonstrate the existence of multiple chemical pathways for CIONO₂ photodissociation. They lead to different photoproducts. However, kinetic studies show that the products grew in concert with an apparent kinetic rate constant nearly equal to the kinetic rate constant of the CIONO₂ decay. This observation suggests that the photodissociation of CIONO₂ could arise from a common excited transient species. This intermediate, not observed in our spectra, could be the CIOONO isomer (16 kcal mol⁻¹ less stable electronically than CIONO₂ [35]) which is expected to decompose considerably faster in the atmosphere [36].

The results of the present study, which may be important in regard to the photochemistry on polar stratospheric cloud particles, are only exploratory at this stage.

Further experiments using pulsed tunable lasers are planned in order (i) to determine if the major gas-phase pathway (4) can account for the origin of CINO formation and (ii) to calculate quantum yields for the different processes at various wavelengths of monochromatic radiation.

Acknowledgement

The authors wish to thank Professor Dizabo for helpful advice on CIONO₂ preparation. They are also grateful to Dr. André Schriver for assistance with experimental devices.

References

- [1] M.B. McElroy, R.J. Salawitch and S.C. Wofsy, *Geophys. Res. Letters* 13 (1986) 1296.
- [2] L.B. Callis and M. Natarajan, *Nature* 323 (1986) 772.
- [3] M.B. McElroy, R.J. Salawitch, S.C. Wofsy and J.A. Logan, *Nature* 321 (1986) 759.
- [4] R.A. Cox, J.P. Burrows and G.B. Coker, *Intern. J. Chem. Kinetics* 16 (1984) 445.
- [5] M.J. Molina, L.T. Tso, L.T. Molina and F.C.Y. Wang, *Science* 238 (1987) 1253.
- [6] W.S. Smith, C.C. Chou and F.S. Rowland, *Geophys. Res. Letters* 4 (1977) 517.
- [7] S.M. Alder-Golden and J.R. Wiesenfeld, *Chem. Phys. Letters* 82 (1981) 281.
- [8] J.S. Chang, J.R. Barker, J.E. Davenport and D.M. Golden, *Chem. Phys. Letters* 60 (1979) 385.
- [9] W.J. Marinelli and H.S. Johnston, *Chem. Phys. Letters* 93 (1982) 127.
- [10] J.J. Margitan, *J. Phys. Chem.* 87 (1983) 674.
- [11] H.D. Knauth and R.N. Schindler, *Z. Naturforsch.* 38a (1983) 893.
- [12] J.P. Burrows, G.S. Tyndall and G.K. Moortgat, *J. Phys. Chem.* 92 (1988) 4340.
- [13] M. Schmeisser, *Inorg. Synth.* 9 (1967) 127.
- [14] G.H. Cady, *Inorg. Synth.* 5 (1957) 156.
- [15] N.S. Gruenhut, M. Goldfrank, M.L. Cushing and G.V. Caesar, *Inorg. Synth.* 3 (1950) 78.
- [16] R.H. Miller, D.L. Bernitt and I.C. Hisatsune, *Spectrochim. Acta* 23A (1967) 223.
- [17] R.D. Suenram and D.R. Johnson, *J. Mol. Spectry.* 65 (1977) 239.
- [18] R.D. Suenram and F.J. Lovas, *J. Mol. Spectry.* 105 (1984) 351.
- [19] J.W. Fleming, *Chem. Phys. Letters* 50 (1977) 107.
- [20] K.V. Chance and W.A. Traub, *J. Mol. Spectry.* 95 (1982) 306.
- [21] D.W.T. Griffith, G.S. Tyndall, J.P. Burrows and G.K. Moortgat, *Chem. Phys. Letters* 107 (1984) 341.
- [22] F.S. Rowland, J.E. Spencer and M.J. Molina, *J. Phys. Chem.* 80 (1976) 2711.
- [23] L.H. Jones and B.I. Swanson, *J. Phys. Chem.* 95 (1991) 86.
- [24] B.M. Cheng, J.W. Lee and Y.P. Lee and Y.P. Lee, *J. Phys. Chem.* 95 (1991) 2814.
- [25] J. Hacıoglu, S. Suzer and L. Andrews, *J. Phys. Chem.* 94 (1990) 1759.
- [26] D.F. Smith Jr., J. Overend, R.C. Spiker and L. Andrews, *Spectrochim. Acta* 28A (1972) 87.
- [27] D. Lucas and G.C. Pimentel, *J. Phys. Chem.* 83 (1979) 2311.
- [28] D.E. Tevault and R.R. Smardzewski, *J. Chem. Phys.* 67 (1977) 3777.
- [29] G.R. Smith and W.A. Guillory, *J. Mol. Spectry.* 68 (1977) 223.
- [30] A. Arkell and I. Schwager, *J. Am. Chem. Soc.* 89 (1967) 5999.

- [31] W. DeMore and O.F. Raper, *J. Chem. Phys.* 37 (1962) 2048.
[32] F. Magnotta and H.S. Johnston, *Geophys. Res. Letters* 7 (1980) 769.
[33] D.E. Tevault and R.R. Smardzewski, *J. Phys. Chem.* 82 (1978) 375.
[34] B.R. Cairns and G.C. Pimentel, *J. Chem. Phys.* 43 (1965) 3432.
[35] S.L. Bathia and J.H. Hall, *J. Chem. Phys.* 82 (1985) 1991.
[36] J.S. Chang, A.C. Baldwin and D.M. Golden, *J. Chem. Phys.* 71 (1979) 2023.